Role of diamagnetic and neoclassical effects in non-linear MHD rotating plasma response to resonant magnetic perturbations

M. Becoulet[1], P. Maget[1], G.T.A. Huysmans[1], X. Garbet[1], E. Nardon[1], A.Smolyakov[2], F. L. Waelbroeck[3], D. Meshcheriakov[1], F. Orain[4,1].

[1] *CEA, IRFM, F-13108, St. Paul-lez-Durance, France.*
[2] *Physics and Engineering Physics Department University of Saskatchewan, 116 Science Place, Saskatoon, SK S7N 5E2, Canada.*
[3] *Institute for Fusion Studies, University of Texas, Austin, TX 78712, USA.*
[4] *PHELMA, Grenoble INP, Minatec, 3 Parvis Louis Néel, BP 257, 38016 Grenoble, France.*

1. Introduction. Resonant Magnetic Perturbations (RMPs) represent one of the promising methods of Type I ELM control in ITER [1]. However, at a level of vacuum ergodisation similar to DIII-D for *r/a >0.9* the application of RMPs demonstrated a variety of ELM responses: ELM suppression [2], ELM mitigation [3], ELM triggering [4] or even no effect on ELMs [5]. This illustrates the present lack of understanding of plasma response, essential for a reliable extrapolation of the RMP method to ITER. In the present work the resistive MHD response to RMPs in a rotating plasma was studied using a non-linear reduced RMHD cylindrical model [6-7]. The model was further developed to include neoclassical and two fluid diamagnetic effects.

2. Model. The fluid velocity for the species *s* (electron and ions) is represented in cylindrical geometry $\{r;\theta;z\}$ similar to [6-7]: $\vec{V}_s \approx \vec{V}_E + \vec{V}_{\parallel,s} + \vec{V}_s^*$, where $\vec{V}_E = \frac{\vec{E}\times\vec{B}}{B^2} \approx -\frac{\nabla\phi\times\vec{e}_z}{B}$, $\vec{V}_{\parallel,s} = \frac{1}{B^2}(\vec{V}_s\vec{B})\vec{B} = V_s\vec{b}$, and $\vec{V}_s^* = \frac{\vec{B}\times\nabla p_s}{e_s n_s B^2} \approx -\frac{\nabla p_s \times \vec{e}_z}{n_s m_s \Omega_{cs}}$. The last term could be important in the pedestal region with steep pressure gradients [8]. Here p is the electron pressure, ϕ the electrostatic potential, electron density $n_e = Zn_i; Z=1$ and $\Omega_{cs} = \frac{e_s B_T}{m_s}$ the cyclotron frequency. Another important factor is the strongly sheared equilibrium radial electric field which exhibits a well-like structure in the pedestal region [9]. This leads to a strong perpendicular rotation $V_{\vec{E}\times\vec{B}}$ in the pedestal and possible additional RMP screening (neglected in [7]). The pressure tensor is now taken in the form: $\mathbf{P}_s = \mathbf{I}p_s + \Pi_s^g + \Pi_s^{neo}$ compared to [7].Here the heuristic form [10] was used: $\nabla\cdot\Pi_s^{neo} \approx n_s m_s \mu_s \frac{B^2}{B_\theta^2}(\vec{V}_s\vec{e}_\theta + k_s\vec{V}_{T,s}\vec{e}_\theta)\vec{e}_\theta$, where $\vec{V}_{T,s} = \frac{\vec{B}\times\nabla T_s}{e_s B^2} \approx -\frac{\nabla T_s \times \vec{e}_z}{m_s\Omega_{cs}}$ and μ_s, k_s are the neoclassical coefficients [10]. This model explicitly supposes that the poloidal ion velocity, averaged over a magnetic surface, in equilibrium tends to its neoclassical value: $\langle V_\theta \rangle = V_\theta^{neo} \approx k_i \frac{1}{m_i\Omega_{ci}}\frac{\partial T_i}{\partial r}$ due to the large neoclassical viscosity [11]. The normalized system of non-linear RMHD equations is solved in a following form:

$$\frac{\partial \psi}{\partial t} = -\eta(J - J_{t=0}) - \nabla_{\parallel}(\Phi - \delta p) \quad (1)$$

$$\frac{\partial W}{\partial t} = \left[W, \Phi + \tau\delta p\right] - \nabla_{\parallel} J + \tau\delta\left[\nabla_{\perp} p, \nabla_{\perp}\Phi\right] + F^{neo}_{\perp,00} + \nu_{\perp}\nabla^2 W \quad (2)$$

$$\frac{\partial p}{\partial t} = \left[p, \Phi\right] - \beta\nabla_{\parallel}(V - 2\delta J) + k_{\perp}\nabla^2(p - p_{t=0}) \quad (3)$$

$$\frac{\partial V}{\partial t} = \left[V, \Phi\right] - \frac{1+\tau}{2}\nabla_{\parallel} p + \delta\tau\beta\frac{1+\tau}{2}\left[p, V\right] + F^{neo}_{\parallel,0,0} + \nu_{\parallel}\nabla^2(V - V_{t=0}) \quad (4)$$

Here ψ is the poloidal flux, p the electron pressure, Φ the electrostatic potential and $V = \frac{1}{B}(\vec{V}_i\vec{B})$ the parallel ion velocity. The parallel gradient is given by $\nabla_{\parallel} S \approx \frac{\partial S}{\partial z} + \left[S, \psi\right]$, $\left[S, \psi\right] \equiv \vec{e}_z \cdot \vec{\nabla}_{\perp} S \times \nabla_{\perp}\psi$, the parallel current density is $J = -\nabla_{\perp}{}^2\psi$ and $W = -\nabla_{\perp}{}^2\Phi$ is the vorticity. The dimensionless parameters are $\delta = \frac{1}{2\Omega_{ci}\tau_A}$, $\beta \equiv \beta_e = \frac{n_e T_e}{B_T^2 / 2\mu_0}$ and τ_A is the Alfven time. The temperature profiles are not evolved in the code, the density is $n_{0,0} = \frac{p_{0,0}}{T_e(r)}$ and $\tau = \frac{T_i}{T_e} = 1$. More detailed description of the equations (1-6) is given in [6]. Normalization [7] is following : $r \to r/a$; $B \to B/B_T$; $\psi \to \psi/a$; $V \to V/V_A$; $t \to t/\tau_A$; $\Phi \to \phi/(V_A B_T a)$

The neoclassical viscosity terms are taken into account in the equations for the values averaged over a magnetic surface (harmonics *n=0, m=0*):

$$F^{neo}_{\perp,0,0} = -\mu^{neo,1}\left\{W_{00} - \frac{1}{r}\frac{\partial}{\partial r}\left(r\left(V_{0,0}\frac{r}{qR_0} + \frac{\tau\delta}{n_{0,0}}\frac{\partial p_{0,0}}{\partial r} + k_i\tau\delta\frac{\partial T_e(r)}{\partial r}\right)\right)\right\} \quad (5)$$

$$F^{neo}_{\parallel,0,0} = -\mu^{neo,2}\left(\frac{\partial \Phi_{0,0}}{\partial r} + V_{0,0}\frac{r}{qR_0} + \frac{\delta\tau}{n_{0,0}}\frac{\partial p_{00}}{\partial r} + \tau\delta k_i\frac{\partial T_e(r)}{\partial r}\right) \quad (6)$$

with $\mu^{neo,1} = \mu^{neo}\left(\frac{qR_0}{r}\right)^2$ $\mu^{neo,2} = \mu^{neo}\frac{qR_0}{r}$. The vacuum amplitudes of the RMP harmonics ψ_{nm} are given at the plasma boundary *r=1* for a magnetic flux perturbation similar to [7].

3. Results. DIIII-D-like parameters [12] were used initially: $R_0 = 1.8m$, $a = 0.6m$; $B_\varphi \sim B_T = 1.9T$, cylindrical $q_{95} \sim 3.15$, central density, temperature, toroidal rotation and resistivity are respectively: $n_{e,0} = 8.10^{19} m^{-3}$, $T_{e,0} = 1.5keV$, $V_{\varphi,0} = 72km/s$, $\eta_0 = 10^{-8}$. For simplification $\mu^{neo,1,2} = 5.10^{-5}$, $\nu_{\parallel} = 10^{-6}$, $\nu_{\perp} = 10^{-8}$, $k_{\perp} = 10^{-5}$, $k_i = -0.8$, δ=0.03 are kept constant. The resistivity profile has a T_e dependence: $\eta \sim T_e^{-3/2}$. Density and temperature profiles are proportional to the $f(r)=0.5(1-\tanh((r-r_{bar})/\sigma)$ with $r_{bar}=0.98$ and a pedestal width $\sim\sigma=0.06$. The strong screening can be seen in Fig.1 for a single island *(n=-3,m=8)*, $\psi_{nm}(1)\sim 5.10^{-5}$. The q_{95} and RMP amplitude scans demonstrated that the vacuum-like size island is formed in a certain resonant window Δq_{95} (Fig.2).The resonant window where RMP

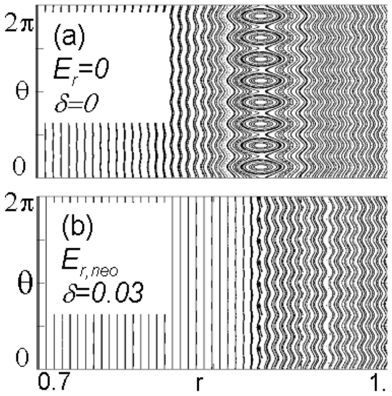

Fig.1. *(a)- Island (8/3) in "vacuum". (b)-screened island (8/3) with diamagnetic effects and neoclassical E_r at $t=10^5\tau_A$*

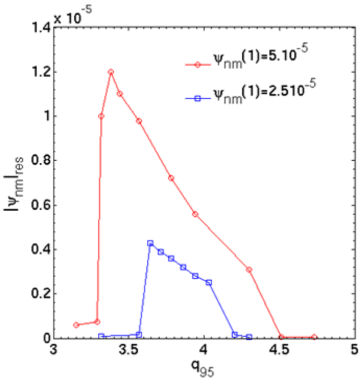

Fig.2. *Maximum RMP amplitude on the resonant surface q=8/3 for single harmonic (m=8,n=-3) in q_{95} and RMP amplitude scans.*

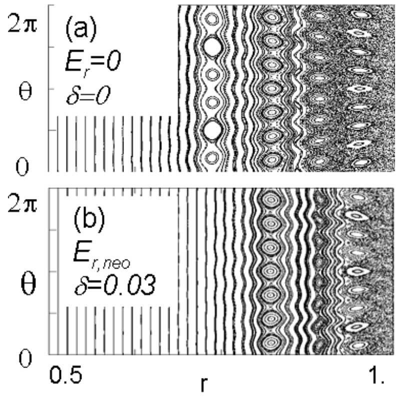

Fig.3. *(a)- Vacuum magnetic topology with RMP spectrum. (b)- the same as (a) but with neoclassical and diamagnetic effects at t=6.10*^{4} *τ_A; q_{95}=3.11*

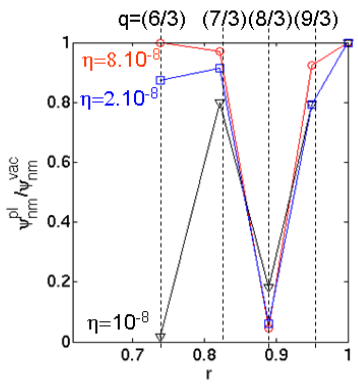

Fig.4. *Screening factor profile $|\psi^{pl}_{nm}/\psi^{vac}_{nm}|$ for RMP edge harmonics in resistivity scan.*

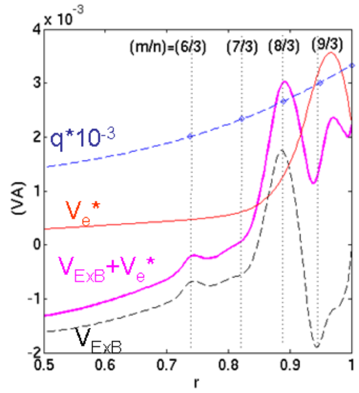

Fig5. *Profiles of V_{ExB} and V_e^* at the edge. The position of resonances q=m/n are indicated by vertical lines.*

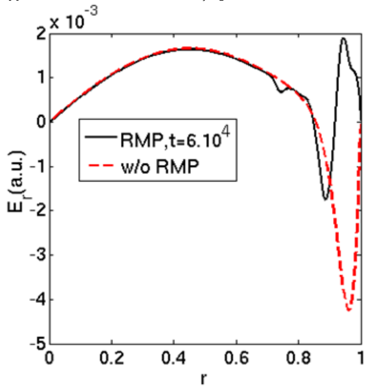

Fig.6. *Radial electric field without RMPs and with RMPs spectrum corresponding to Fig.3*

penetrate is about Δq_{95} *~1.-0.5* and decreases for smaller RMP amplitudes (Fig.2). Analysis similar to [13,14] showed that the RMP penetration happens where the $\vec{E}\times\vec{B}$ poloidal rotation is compensated by the electron diamagnetic rotation $V_{\vec{E}\times\vec{B}}+V_e^*\sim 0$. This corresponds to the cancelation of the second term in the right hand side of Ohm's law, equation (1). The magnetic topology resulting from the RMP spectrum $\psi_{n=-3;m=6,7,..10}(1)=(8,7,...4)\times 10^{-5}$ (Fig.3) shows strong central screening of RMPs except for the island *(7/3)*. The RMP screening is stronger for lower resistivity and stronger rotation (including diamagnetic) [15, 7] which is illustrated in Fig.4. Notice (Fig.5) that the condition $V_{\vec{E}\times\vec{B}}+V_e^*\sim 0$ is satisfied for the island *(7/3)*, which explains why it is not screened. The radial electric field E_r is more positive in the presence of RMPs and its minimum moves more inside (Fig.6) which reminds experimental observations [9]. Modeling of the magnetic topology with RMPs for an ITER-like case: $R_0 = 6m$, $a = 2m$, $B_T = 5.3T$, $q_{95} \sim 3.1$, $n_{e,0} = 10^{20} m^{-3}$, $T_{e,0} = 20keV$, $V_{\varphi,0} = 6km/s$, $\eta_0 = 0.510^{-8}$, $k_i = -1.$, *δ=0.009*, and $\psi_{n=-4;m=9:13}(1) = 5.10^{-5}$ is shown in (Fig.7). Notice that compared to the DIII-D case there is no point where $V_{\vec{E}\times\vec{B}} + V_e^* \sim 0$ (Fig.8).

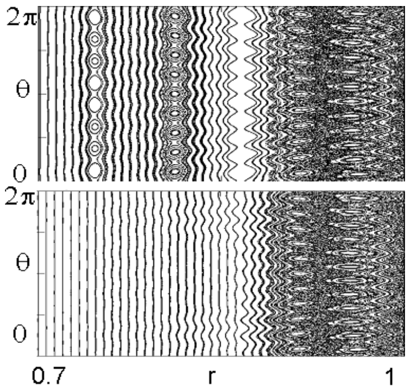

Fig.7 Similar to Fig.3 but for ITER-like parameters.

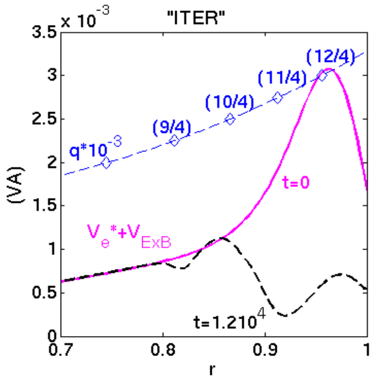

Fig.8 *Poloidal velocity evolution due to RMPs in ITER.*

However, in the present modelling the poloidal velocity (and hence the RMP screening), decreases due to the non-linear effect of RMPs on the edge radial electric field (more positive with RMPs) leading to increased RMP penetration.

Conclusions. The RMHD model with diamagnetic and neoclassical effects was applied to the case of RMP penetration into the pedestal region. The RMP screening, increasing at lower resistivity, was demonstrated in the zone of steep pedestal gradients due to strong poloidal rotation $V_{\vec{E}\times\vec{B}} + V_e^*$. Narrow *($\Delta q_{95}$~1-0.5)* RMP penetration windows (smaller for smaller RMP amplitude) exist at certain parameters in a region where the poloidal rotation is compensated by the electron diamagnetic rotation $V_{\vec{E}\times\vec{B}} + V_e^* \sim 0$.

This work, supported by the European Communities under the contract of Association between EURATOM and CEA, was carried out within the framework of the European Fusion Development Agreement. The views and opinions expressed herein do not necessarily reflect those of the European Commission.

References:

[1] R Hawryluk et al. Nucl. Fus **49** (2009)065012
[2] M Fenstermacher et al Phys of Plas**15**(2008)56122
[3] Y. Liang et al Phys Rev Letters **98** (2007)265004
[4] J M Canik et al Nucl Fusion **50**(2010)034012
[5] A Kirk et al Nucl Fusion **50**(2010)034008
[6] R D Hazeltine Phys Fluids **28**(1985)2977
[7] M Becoulet et al Nucl Fusion **49**(2009)085011
[8] D Reiser et al Phys. Plasmas **16** (2009) 042317
[9] K Burrell et al Plasma Phys. Cont Fusion **47** (2005) B37
[10] T Gianakon et al Physics of Plas, 9(2002) 536
[11] A Smolyakov Phys of Plasmas **11**(2004) 4353
[12] T Osborne et al., Proc. 32nd EPS Conf. Plasma Physics, Tarragona (2005) P4.012
[13] E Nardon et al Nucl Fusion **50**(2010)034002
[14] F L Waelbroeck Phys. Plasmas **10** (2003) 4040
[15] R Fitzpatrick *Phys. Plasmas* **5** (1998) 3325